




## PD-L1 expression is a prognostic factor in subgroups of gastric cancer patients stratified according to their levels of CD8 and FOXP3 immune markers

Le Ying <sup>a,b,c</sup>, Feng Yan <sup>a,b</sup>, Qiaohong Meng<sup>b</sup>, Liang Yu<sup>d</sup>, Xiangliang Yuan<sup>a</sup>, Michael P. Gantier <sup>e</sup>, Bryan R. G. Williams<sup>e</sup>, David W. Chan<sup>f</sup>, Liyun Shi<sup>g</sup>, Yugang Tu<sup>h</sup>, Peihua Ni<sup>a</sup>, Xuefeng Wang<sup>a</sup>, Weisan Chen<sup>i</sup>, Xingxing Zang<sup>j</sup>, Dakang Xu<sup>a,b,e</sup>, and Yiqun Hu<sup>a</sup>

<sup>a</sup>Faculty of Medical Laboratory Science, Ruijin Hospital, School of Medicine, Shanghai Jiao Tong University, Shanghai, P. R. China; <sup>b</sup>Institute of Ageing Research, Hangzhou Normal University School of Medicine, Hangzhou, P. R. China; <sup>c</sup>Department of Tea Science, Zhejiang University, Hangzhou, P. R. China; <sup>d</sup>Department of General Surgery, Shanghai Jiao Tong University Affiliated First People's Hospital, Shanghai, P. R. China; <sup>e</sup>Hudson Institute of Medical Research, Department of Molecular and Translational Science, Monash University, Clayton, Victoria, Australia; <sup>f</sup>Department of Obstetrics and Gynaecology, LKS Faculty of Medicine, The University of Hong Kong, Hong Kong SAR, P. R. China; <sup>g</sup>Department of Microbiology and Immunology, Nanjing University of Chinese Medicine, Nanjing, P. R. China; <sup>h</sup>Cell Signaling Technology, Inc., Asia Pacific; <sup>i</sup>La Trobe Institute for Molecular Science, La Trobe University, Bundoora, Victoria, Australia; <sup>j</sup>Department of Oncology, Montefiore Medical Center, Albert Einstein College of Medicine, Bronx, NY; Department of Microbiology and Immunology, Albert Einstein College of Medicine, Bronx, NY; Department of Medicine, Montefiore Medical Center, Albert Einstein College of Medicine, Bronx, NY, USA

### ABSTRACT

Current studies aiming at identifying single immune markers with prognostic value have limitations in the context of complex antitumor immunity and cancer immune evasion. Here, we show how the integration of several immune markers influences the predictions of prognosis of gastric cancer (GC) patients. We analyzed Tissue Microarray (TMA) by multiplex immunohistochemistry and measured the expression of immune checkpoint molecule PD-L1 together with antitumor CD8 T cells and immune suppressive FOXP3 Treg cells in a cohort of GC patients. Unsupervised hierarchical clustering analysis of these markers was used to define correlations between CD8 T, FOXP3 Treg and PD-L1 cell densities. We found that FOXP3 and PD-L1 densities were elevated while CD8 T cells were decreased in tumor tissues compared to their adjacent normal tissues. However, patient stratification based on each one of these markers individually did not show significant prognostic value on patient survival. Conversely, combination of the ratios of CD8/FOXP3 and CD8/PD-L1 enabled the identification of patient subgroups with different survival outcomes. As such, high densities of PD-L1 in patients with high CD8/FOXP3 and low CD8/PD-L1 ratios correlated with increased survival. Collectively, this work demonstrates the need for the integration of several immune markers to obtain more meaningful survival prognosis and patient stratification. In addition, our work provides insights into the complex tumor immune evasion and immune regulation by the tumor-infiltrating effector and suppressor cells, informing on the best use of immunotherapy options for treating patients.

### ARTICLE HISTORY

Received 16 November 2017  
Revised 22 January 2018  
Accepted 22 January 2018



### KEYWORDS


Clustering analysis; gastric cancer; multiplexed immunohistochemistry; prognostic

## Introduction

Gastric cancer (GC) is the most significant malignancy in Asian populations and is associated with significant mortality. In spite of novel insights into the molecular basis of GC, current available therapies do not significantly improve the overall patient survival (OS). Using disease risk stratification based on tumor size, lymph node or distant metastases (TNM staging) and histological grading is not sufficient for the prognosis of individual GC patients.<sup>1</sup> Additional prognostic biomarkers are urgently needed. The tumor-infiltrating immune cells have been proposed to have prognostic value and are a major component of assessing the therapeutic outcome of various treatments, especially immunotherapy.<sup>2</sup> As such, T cells play critical roles in the

control of tumor development and nodal metastasis; and their capacity to produce antitumor cytokines was found to be decreased in patients with high tumor burden and lymph node metastasis.<sup>3</sup> Such immune dysfunction in the tumor environment correlates with poorer patient survival.<sup>4</sup> We and others have previously discovered that GC tissues exhibited a reduced frequency and activity of immune effector cells (largely CD8 T cells) and increased frequency of regulatory T cells (Treg).<sup>5-7</sup> How the activity of these tumor infiltrating immune cells relates to GC development and disease prognosis is however poorly defined. So far, detailed analysis on immune cell infiltration, tumor immune escape and their correlation with clinical parameters are rare, knowing that immunosuppressive mechanisms

**CONTACT** Dr. Yiqun Hu  [ichunhu@126.com](mailto:ichunhu@126.com)  [dakang.xu@monash.edu](mailto:dakang.xu@monash.edu)

 Supplemental data for this article can be accessed on the [publisher's website](#).

Le Ying and Feng Yan contributed equally to this work.

© 2018 Le Ying, Feng Yan, Qiaohong Meng, Liang Yu, Xiangliang Yuan, Michael P. Gantier, Bryan R. G. Williams, David W. Chan, Liyun Shi, Yugang Tu, Peihua Ni, Xuefeng Wang, Weisan Chen, Xingxing Zang, Dakang Xu, and Yiqun Hu. Published with license by Taylor & Francis Group, LLC

This is an Open Access article distributed under the terms of the Creative Commons Attribution-NonCommercial-NoDerivatives License (<http://creativecommons.org/licenses/by-nc-nd/4.0/>), which permits non-commercial re-use, distribution, and reproduction in any medium, provided the original work is properly cited, and is not altered, transformed, or built upon in any way.

within the tumor microenvironment are associated with the dysfunction of tumor-infiltrating lymphocytes (TILs).<sup>8</sup>

Studies using quantitative immunohistochemistry (IHC) have shown that tumor-infiltrating CD8 T cell number (abundance) is an important prognostic parameter in predicting GC patient survival,<sup>9</sup> suggesting that CD8 T cells might be used as a single biomarker in GC. Nonetheless, the intratumoral presence of CD8 T cells does not necessarily mean that they can exert direct anti-tumor activities. Indeed, the function of intratumoral CD8 T cells is controlled by FOXP3 Treg cells and by immunosuppressive ligands such as programmed death-ligand 1 (PD-L1).<sup>10</sup> As such, FOXP3 Tregs play a critical role in tumor immune evasion,<sup>5</sup> which has been reported in a wide array of human malignancies including GC.<sup>5,6</sup> Accordingly, an increase of intratumoral FOXP3 Tregs is associated with reduced CD8 T cell tumor infiltration and worse outcomes for cancer patients.<sup>11</sup> However, a detailed quantitative understanding of the dynamic relation between tumor-infiltrating CD8 T cells and those expressing PD-L1, and FOXP3 Tregs, and their potential as immune and prognostic biomarkers remains to be clearly established in GC.

In this study, we analyzed three key immune marker expression including checkpoint molecule PD-L1, antitumor T cell marker CD8 and immune suppressive Treg marker FOXP3 as well as their potential prognostic value in GC. More specifically, relying on multiplex immunohistochemistry (mIHC) of formalin-fixed paraffin-embedded (FFPE) tumor tissue microarrays (TMAs), we explored the relationship between these markers in cancer tissues and their adjacent normal tissues derived from 84 GC patients, and related such data to disease prognosis, patient survival and stratification. Moreover, our patient clustering approach was validated using an RNAseq dataset from a TCGA cohort.

## Methods

### Sample and tissue microarray preparation

GC tissues were obtained from Shanghai Jiao Tong University, Ruijin Hospital. These tissues were formalin-fixed and paraffin-embedded. All protocols using human specimens were approved by Shanghai Jiao Tong University Human Ethics Committee, and informed consent was obtained from all patients. One TMA included 180 GC tissues from patients (90 paired tumor and adjacent normal tissues), but 12 samples (6 paired tumor and adjacent normal tissues) were excluded due to incompleteness of the tissues. Detailed information is shown in Supplementary Table S1. TMAs were made based on pathology diagnosis of each tissue. The blocks were assembled and an independent surgical pathologist reviewed the H&E slide for each case. The pathologist then circled the area of the block, localizing a representative tumor region from which a core was extracted for our TMAs. Then we applied H&E staining on TMAs to validate pathology type of each tissue on each TMA, and the results of H&E staining are shown in Supplementary Fig S1. The core diameter on each TMA in this study was 1.5 mm, which was much larger than the normal TMA core (0.6 mm),<sup>12</sup> to provide more representative tissues on TMA.

## Immunohistochemistry

GC paraffin blocks were processed into four-micrometer-thick sections and mounted on slides for staining. First, the slides were deparaffinized in xylene using ethanol series (75%, 50%, 25%). Antigen recovery was performed by microwaving the samples for 15 min in citrate buffer (pH 6.0), and the slides were cooled for 30 min. Endogenous peroxidases were then blocked by treating the tissues with 3% H<sub>2</sub>O<sub>2</sub> for 10 min. Then, the tissues were incubated with blocking serum for 20 min at room temperature. Afterwards, the slides were incubated overnight with anti-CD8 (1:500 dilution in SignalStain Antibody Diluent), anti-PD-L1 (1:250 dilution in SignalStain Antibody Diluent), and anti-FOXP3 (1:350 dilution in SignalStain Antibody Diluent) primary antibodies (Cell Signaling, USA) respectively at 4 °C and incubated with horseradish peroxidase (HRP) (Vectastain ABC kit, USA) for 30 min on the next day. The slides were incubated with ABC reagent (Vectastain ABC kit, USA) for another 30 min at room temperature, washed with TBST, and stained with 3, 3'-diaminobenzidine (DAB). Finally, the slides were counterstained with hematoxylin and mounted with coverslips in DPX (Sigma, USA) for imaging. All staining preparations included a non-primary-antibody control, details are described by previous studies.<sup>12,13</sup>

### Multiplex immunohistochemistry

For mIHC staining, a PD-L1, FOXP3 and CD8 $\alpha$  multiplex IHC antibody panel kit (Cell Signaling, USA) and Opal 4-color fluorescent IHC kit (PerkinElmer, USA) were used.<sup>14</sup> First, the concentration and the application order of the three antibodies were optimized, and the spectral library was built based on the single-stained slides. The slides were first deparaffinized by xylene and ethanol (Concentration of 100%, 75%, 50% and 25%) and antigen retrieval was performed by microwave. After incubating with 3% H<sub>2</sub>O<sub>2</sub> (freshly made) for 10 mins, the tissues were blocked in blocking buffer for another 10 mins at room temperature. Then the tissues were incubated by primary antibody (Cell signaling, USA), secondary-HRP (Cell signaling, USA) and Opal working solution (PerkinElmer, USA). The slides then were mounted with ProLong Gold Antifade Reagent with DAPI (Cell signaling, USA).

### Evaluation of immunostaining

All the slides were scanned using a Nikon C1 confocal microscope (Nikon, Japan). The Nikon C1 confocal microscope produces virtual images of full tissue scans which can be analyzed visually as well as automatically using image processing algorithms. The full tissue sections allow large scale histological evaluations with high precision across the complete section, which can avoid the ambiguity caused by variable cell densities in different parts of the tissues. The positive stained CD8 and FOXP3 cell numbers per mm<sup>2</sup> and the average intensity of PD-L1 per mm<sup>2</sup> were analyzed by ImageJ software (ImageJ 1.51 n, National institutes of health, USA). All these results were described as the density (cells per mm<sup>2</sup>) of positive stained cells in the following analysis. The detailed protocol is described in the Supplementary Methods.

### RNA-seq and clinical information data from TCGA

We used publicly available TCGA data in this study, clinical information and mRNA expression data were downloaded from the NCI's Genomic Data Commons (GDC) portal (<https://portal.gdc.cancer.gov>). Raw RNA-seq count matrix and clinical information were obtained using TCGA Bioinformatics (2.5.7) package in R (3.4.0). The count matrix was transformed into log<sub>2</sub> count per million (lcpm) using edgeR (3.18.1) package. Lcpm values of *CD274* (*PD-L1*), *CD8 A* (*CD8*) and *FOXP3* RNA were extracted, and the ratio of *CD8 A* to *CD274* and *CD8 A* to *FOXP3* was calculated by deducting lcpm value of corresponding genes. TCGA-STAD cohort contained 32 normal and 375 tumor samples. We used the tumor samples to obtain hierarchical clustering of the patients using two different combinations of predictors, similar to our TMA data analysis. The first combination relied on the 3 single predictors including FOXP3, CD8 and PD-L1. The second combination relied on the 2 ratios including CD8/FOXP3 and CD8/PD-L1.

### Hierarchical clustering analysis

Hierarchical clustering was used to define subgroups of GC patients both in TMA and TCGA cohorts. We used densities of CD8, FOXP3 and intensity of PD-L1 expression along with ratios of CD8/FOXP3 and CD8/PD-L1 as predictors in the TMA cohort. The expression and ratios were log<sub>2</sub> transformed and Euclidean distance was calculated to plot the heatmaps. The tumor samples in the TMA cohort were sub-divided into 3 clusters.

Raw mRNA counts of CD8, FOXP3 and PD-L1 from the TCGA cohort were used to calculate the ratios of CD8/FOXP3 and CD8/PD-L1. The mRNA counts and their ratios were also log<sub>2</sub> transformed (e.g lcpm), and Euclidean distance was calculated to plot the heatmaps. The expression was indicated from red (high level) to blue (low level). Heatmaps and hierarchical clusters were generated in Rstudio (Version 3.2.0), as described in our previous studies.<sup>13,15</sup> The tumor samples in the TCGA cohort were sub-divided to mirror those from the TMA cohort. We found  $k = 5$  gave best representation of the three clusters corresponding to TMA cohort.

### Kaplan–Meier survival curve

The Kaplan–Meier survival curve and p values were generated using survminer (0.4.0) package. In each cluster, we divided the samples into two subgroups by the median value of expression or ratio. The samples in each cluster were fitted to the Cox proportional hazard model to test if it violates the assumption. In case where the proportional hazard model agreed, Log rank test was used to calculate p value. Otherwise, we used Fleming–Harrington test ( $p = 1$ ,  $q = 1$ ) to adjust the p value.

### Statistical analyses

Statistical analyses were carried out using the Kruskal–Wallis test for nonparametric analysis in GraphPad Prism (Version 5.0), and differences were considered statistically significant at  $p < 0.05$ .

## Results

### Differential expressions pattern of CD8, FOXP3 and PD-L1 in GC

We have developed a novel multiplex immunolabelling protocol with a Tyramide Signal Amplification (TSA) signaling, using Opal fluorophores (Supplementary Table S2), which allows for the simultaneous evaluation of 4 markers in a single tissue section. We assessed the concurrent densities of CD8 T cells, FOXP3 Treg cells and PD-L1 cells in tumor tissues and adjacent normal tissues, relying on a 4-color mIHC staining of the TMA samples (Fig. 1 A–D). The PD-L1 was detected in the cell membrane and cytoplasm and was visible in tumor, stromal, and immune cells, but not in non-neoplastic gastric epithelium (Supplementary Fig S2). We also compared tumor tissues (Fig. 1E) to adjacent normal tissues from the same patient (Fig. 1F). Two predominant patterns of immune infiltration were observed in our cohort: tumors with extensive immune infiltration showed high PD-L1 and FOXP3 densities of staining (Fig. 1G); and those with limited immune infiltrates were associated with low PD-L1 and FOXP3 positive cells (Fig. 1H).

### Decreased CD8 /FOXP3 and CD8 /PD-L1 cell densities ratios were detected in GC tumors

We initially compared the densities of CD8 T cells, FOXP3 Treg cells and PD-L1 cells between the GC tissues and paired adjacent normal tissues. We found an increase in densities of FOXP3 and PD-L1 in tumor tissues ( $p < 0.01$ ) (Fig. 2A, B). This contrasted with the significantly decreased densities of CD8 in these tumor tissues ( $p < 0.01$ ) (Fig. 2C). Next, we evaluated the ratios of CD8 to FOXP3 densities. Adjacent normal tissues exhibited a significantly higher CD8/FOXP3 ratio compared with that in the GC tissues (Fig. 2D). Similarly, although not statistically significant, CD8 /PD-L1 ratios were often increased in adjacent normal tissues compared with those in GC tissues (Fig. 2E). These results collectively indicated the immunosuppressive roles of FOXP3 Treg cells and PD-L1 expressed cells, likely expressed on tumor cells and other tumor-infiltrating immune cells in tumor microenvironment.

### The relation of CD8 T, FOXP3 Treg and PD-L1 expressed cells in GC

PD-L1 expressed cells suppress T cell function and induce local immune suppression, and they are often associated with poorer prognosis and poorer patient survival in many cancers including GC.<sup>16</sup> We therefore set out to determine whether there is any relation between PD-L1, CD8 and FOXP3 expressing cells patterns (or densities of positive cells per mm<sup>2</sup> or intensity of per mm<sup>2</sup>). We first divided the GC samples into two groups according to PD-L1 expressing cell densities (PD-L1 expression high and low) based on the median of PD-L1 expression. We next compared the densities of CD8, FOXP3 and the ratio of CD8/FOXP3 cells between the two groups. The density of CD8 T cells and FOXP3 Treg cells were significantly higher in PD-L1 high expression group (Fig. 3A, B). As shown in Fig. 3C, there was significant positive correlation between the

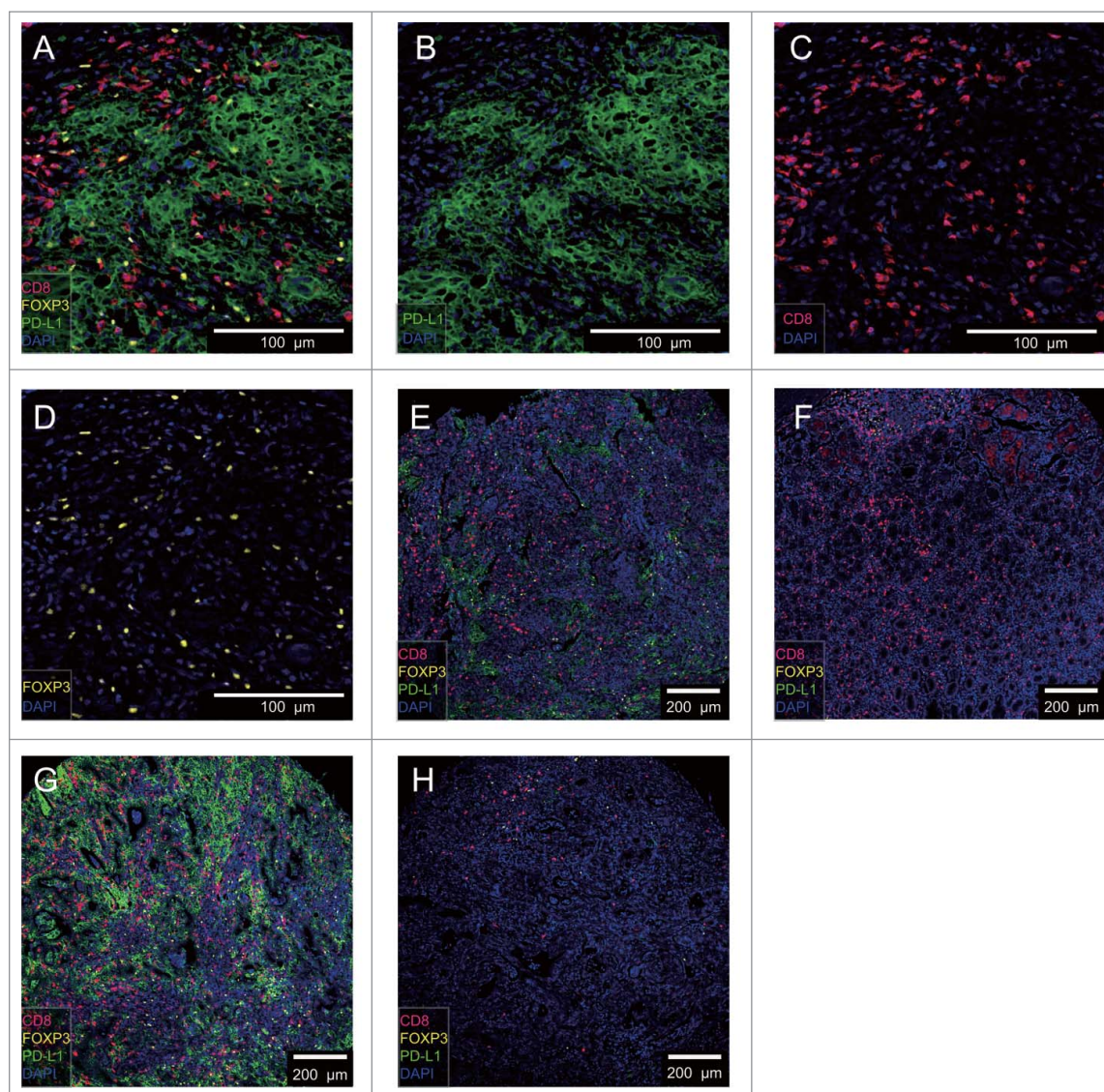


**Figure 1.** 4-color mIHC staining images of different GC tissues. A. Representative 4-color mIHC staining of GC tissue is shown. B. PD-L1 expressed cells were visualized using the FITC channel (green). C. CD8 T cells were visualized using the Cy5 channel (red). D. FOXP3 Treg cells were visualized using the Cy3 channel (yellow). E. Representative image of GC tumor tissue. F. Representative image of GC adjacent normal tissue (E and F sample from the same patient). G. Representative image of GC tissue with abundant CD8 T, FOXP3 Treg and PD-L1 expressed cell infiltration. H. Representative image of GC tissue with minimum CD8 T, FOXP3 Treg and PD-L1 expressed cell infiltration. DAPI was used to visualize nuclei (blue).

density of CD8 cells and FOXP3 Treg cells in GC tissues ( $r = 0.594$ ,  $p < 0.01$ ). Moreover, the density of FOXP3 Treg cells and CD8T cells were also positively correlated with the PD-L1 expression ( $r = 0.386$ ,  $p < 0.01$ , and  $r = 0.473$ ,  $p < 0.01$ , respectively) (Fig. 3D, E), suggesting that PD-L1 expressed cells may play their role on impacting both tumor-reactive and immune suppressive cell populations.

#### **Individual use of CD8, FOXP3 and PD-L1 does not have prognostic value in GC**

We next studied whether using the density levels of CD8 T cells, FOXP3 Treg cells and PD-L1 expressed cells could help refine subgroups of GC patients. Heatmap and clustering analyses were performed to assess the potential correlation between different gastric tumor and adjacent normal tissues. Hierarchical clustering analyses using densities of CD8, FOXP3 and

intensity of PD-L1 expression were applied to generate several subgroups of patients. However, we were unable to distinguish immune signature subgroups between tumor and adjacent normal groups with individual predictor of CD8 T cells, FOXP3 Treg cells and PD-L1 cells for such clustering analyses (Fig. 4A). In line with this, Kaplan-Meier analyses carried out on the entire patient cohort showed that the individual parameter of CD8T, FOXP3 Treg cells and PD-L1 expressed cells did not have significant prognostic value on patients' survival (Fig. 4 B, C, D).

#### **CD8/FOXP3 and CD8/PD-L1 ratios signature separates GC samples between tumor and adjacent normal tissue groups**

In contrast to the above-mentioned results, we were able to segregate the samples into two groups correlating with their origin

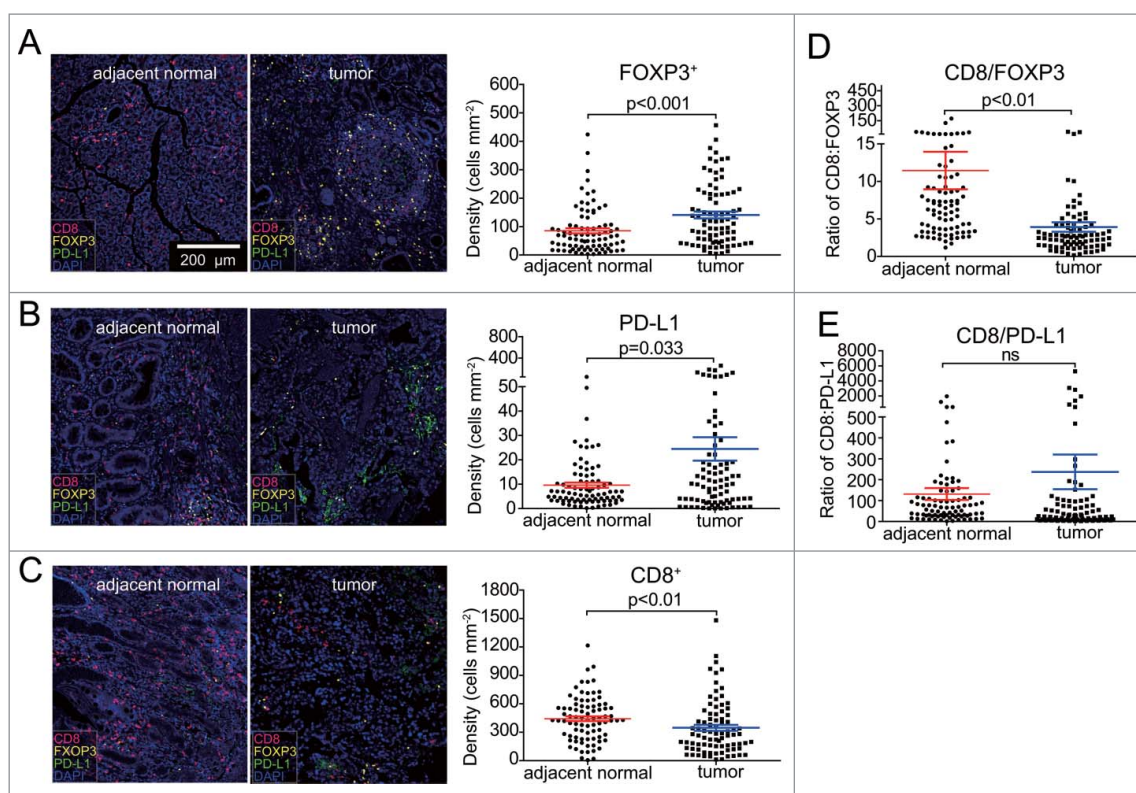


**Figure 2.** Comparison of densities in CD8T, FOXP3 Treg, and PD-L1 cell, CD8/FOXP3 and CD8/PD-L1 expression ratios in tumor and adjacent normal tissues. A. The densities of FOXP3 Treg cells was significantly increased in tumor samples compared to adjacent normal samples ( $p < 0.001$ ). B. The expression of PD-L1 was significantly increased in tumor tissues compared to adjacent normal tissues ( $p < 0.05$ ). C. The levels of CD8T cells (densities) were significantly reduced in tumor areas compared to adjacent normal tissues ( $p < 0.01$ ). D. The CD8/FOXP3 ratio was significantly decreased in tumor tissues compared to adjacent normal tissues ( $p < 0.01$ ). E. CD8/PD-L1 ratio in tumor and adjacent normal tissues was found not significantly different. Error bars represent SEM.

(tumor or adjacent normal tissues), when CD8/FOXP3 and CD8/PD-L1 cell densities ratio were used to perform hierarchical clustering of the samples (Fig. 4E). One group contained most of the GC tissues and mainly displayed low CD8/FOXP3 and CD8/PD-L1 cell ratios, as shown in Fig. 4E. The other

group, associated with adjacent normal tissues, exhibited relatively high ratios of CD8/FOXP3 and CD8/PD-L1. Next, tumor tissues were further stratified into three subgroups according to their ratios of CD8/FOXP3 and CD8/PD-L1 (Fig. 4F). However, Kaplan-Meier analyses showed that separation of GC

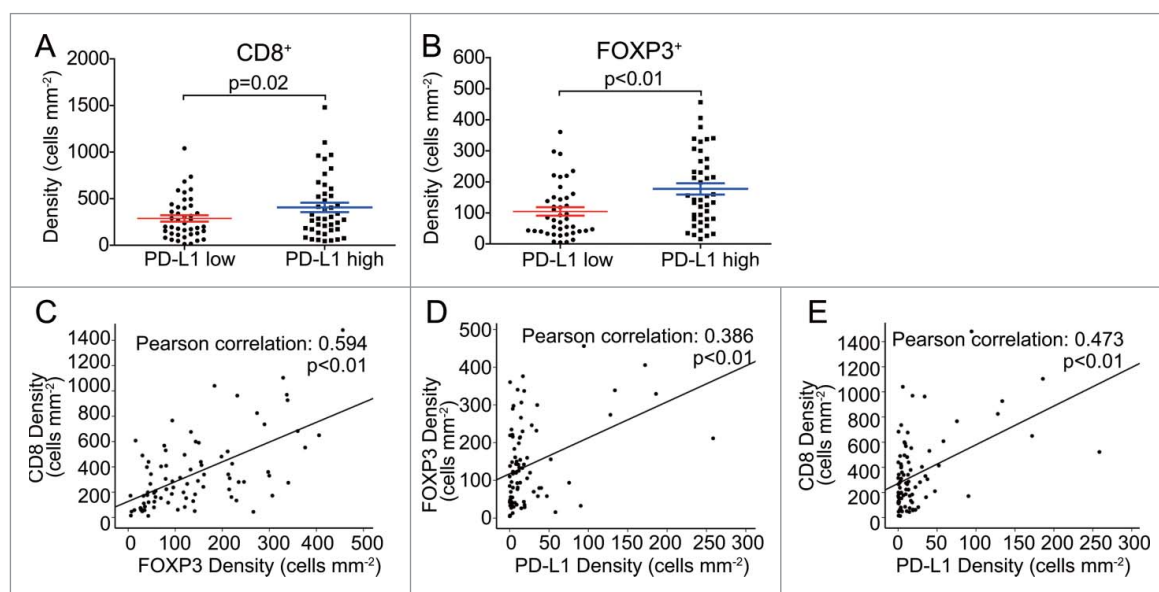


**Figure 3.** Independent analysis and correlation of CD8T, FOXP3 Treg and PD-L1 cells in GC tissues. A-B. Significantly different densities of CD8T and FOXP3 Treg cell were detected in GC tissues of PD-L1 low or high densities group ( $p < 0.05$ ). C-E. Scatter plots of significant correlations, Data are represented in a scattered plot for densities of CD8 and FOXP3, FOXP3 and PD-L1, CD8 and PD-L1 with the best fit line shown ( $n = 84$  for tumor tissues). Correlation coefficient ( $r$ -value) and  $p$ -value of Pearson's correlation test is given on top of each panel. Error bars represent SEM.

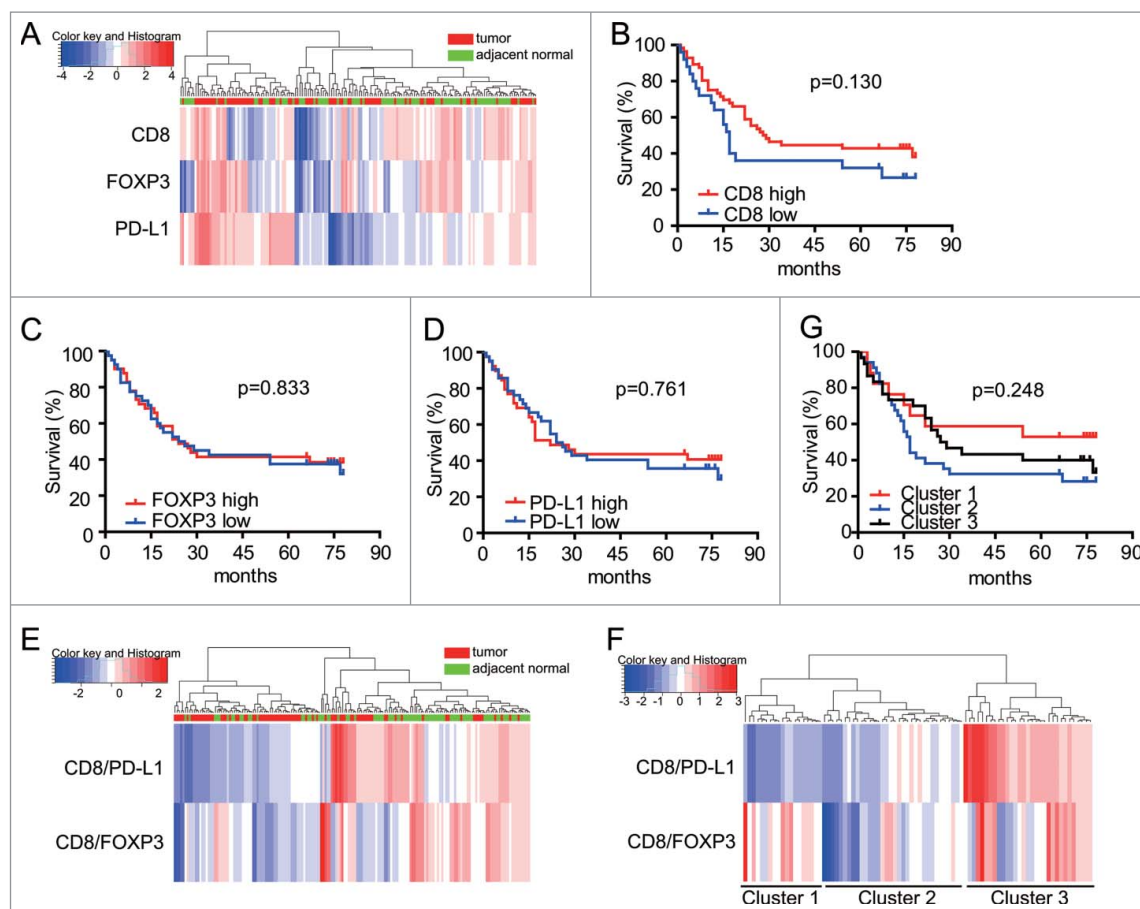


**Figure 4.** Quantitation of densities in CD8, FOXP3 and PD-L1 cells enables patient stratification with prognostic value. A. Heatmap representation of hierarchical clustering of CD8, FOXP3 and PD-L1 density levels is shown, along with a dendrogram of unsupervised hierarchical clustering, for tumor and adjacent normal samples. B-D. Kaplan-Meier curves illustrating the prognostic effect on overall survival (OS) of expression of CD8, FOXP3 and PD-L1 levels of densities for each marker in the cohort of 84 GC patients. A median cutoff was used to separate high and low populations. Log rank test was used to determine significance. CD8/PDL1 and CD8/FOXP3 based subgrouping enables patient stratification with prognostic value. E. Hierarchical clustering of CD8/FOXP3 and CD8/PD-L1 ratios in tumor and adjacent normal samples. F. Hierarchical clustering of CD8/FOXP3 and CD8/PD-L1 in tumor samples only. G. Kaplan-Meier curves illustrating the prognostic effect on overall survival (OS) of three clusters of patients generated according to CD8/PDL1 and CD8/FOXP3 ratios of checkpoint markers, based on Fig. 4F.

patients on the basis of these three subgroups did not allow for survival prediction (Fig. 4G, middle of right panel).

#### ***PD-L1 is a prognostic marker of survival in patients with high CD8/FOXP3 and low CD8/PD-L1 ratios***

In a previous study of GC patients, high levels of PD-L1 in tumors were found to be negatively correlated with patient prognosis.<sup>17</sup> However, our multivariate analyses failed to find significant survival differences based on PD-L1 expressing cells alone (Fig. 4D). We next tested the hypothesis that differences may be observed using subgroups of patients. Accordingly, we analyzed three sub-groups stratified according to the ratios of CD8/PD-L1 and CD8/FOXP3 in tumors samples (based on Fig. 4F), and evaluated the prognostic differences of PD-L1 expressed cells in these groups. High expression of PD-L1 was a significant prognostic factor in the Cluster 1 (exhibiting high ratio of CD8/FOXP3 and low ratio of CD8/PD-L1) (Fig. 5A). However, in the other two groups (Cluster 2: low CD8/FOXP3 ratio and low CD8/PD-L1 ratio; Cluster 3: high CD8/FOXP3 and high CD8/PD-L1 ratios) PD-L1 levels did not show prognostic value (Fig. 5B, C). In addition, CD8 levels did not show prognostic value in any of the subgroups studied (Fig. 5D, E, F).

The prognostic value of PD-L1 levels in patients with high CD8/FOXP3 and low CD8/PD-L1 ratio might indicate blunted immune surveillance in these patients.

#### ***Low CD8/FOXP3 and high CD8/PD-L1 ratios also correlate with better survival outcomes***

The effect of PD-L1 on CD8T-cell function through FOXP3 cells remains to be clarified, but our study indicated that there were no significant correlations between tumor infiltrating CD8T lymphocytes and the patients' survival rates (Fig. 4B). The prognostic value of tumor infiltrating CD8T cells for cancer is controversial. High levels of tumor infiltrating CD8T are thought to be a good predictor of patient survival for a diverse set of human cancers, including gastric and ovarian cancer.<sup>18,19</sup> However, when evaluating the prognostic value of CD8/FOXP3 ratios in the three subgroups of patients described above (i.e. Cluster 1: high CD8/FOXP3 and low CD8/PD-L1; Cluster 2: low CD8/FOXP3 and low CD8/PD-L1; and Cluster 3: high CD8/FOXP3 and high CD8/PD-L1) (Fig. 5G-L), low ratios CD8/FOXP3 were found to be predictive of increased survival in patients from Cluster 3 (Fig. 5I), but not in the other subgroups (Fig. 5G, H). Conversely, CD8/PD-L1 ratios did not

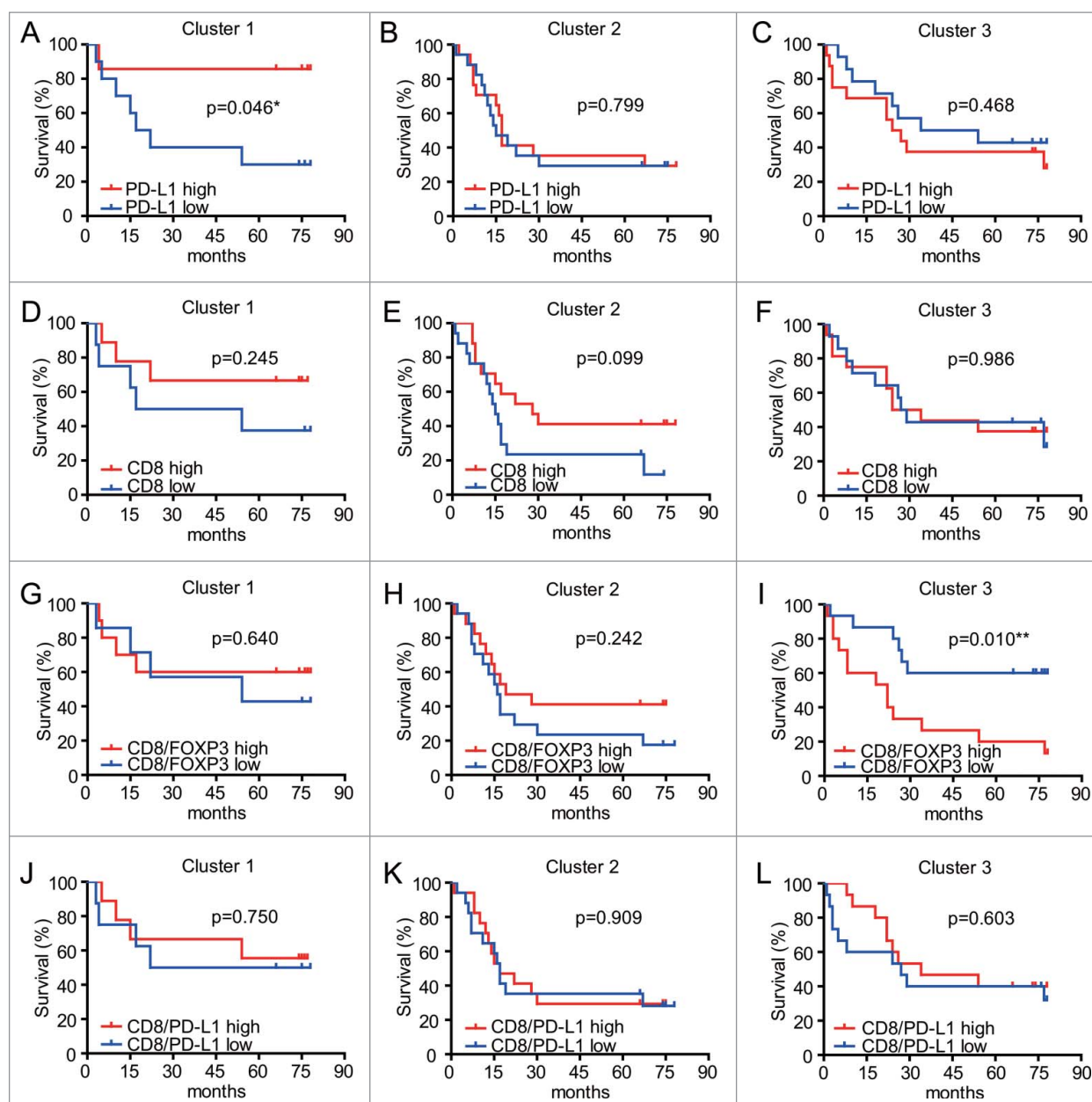


**Figure 5.** Kaplan-Meier analyses of overall survival (OS) for CD8/FOXP3 and CD8/PD-L1 in subgroups of patients based on CD8 or PD-L1 levels. A-C. Survival outcomes of the 84 GC with different expression of PD-L1 from 3 clusters generated according to their CD8/FOXP3 and CD8/PD-L1 ratios. Patients with higher PD-L1 expressions in Cluster 1 had significantly better survival ( $p < 0.05$ ). D-F. Survival outcomes of the 84 GC with different expression of CD8 in the 3 clusters. Kaplan-Meier analyses of overall survival (OS) for CD8/FOXP3 and CD8/PD-L1 in subgroups of patients. G-I. Survival outcomes of the 84 GC patients with different expression of CD8/FOXP3 in the 3 clusters. Patients with lower CD8/FOXP3 levels in Cluster 3 had significantly better survival ( $p < 0.05$ ). J-L. Survival outcomes of the 84 GC patients with different expression of CD8/PD-L1 in the 3 clusters. A-L. A median cutoff was used to separate high and low densities. Statistical analyses were generated using Log rank test.

have prognostic value in any of the subgroups of patients (Fig. 5J, K, L). The results demonstrated that CD8 levels can have prognostic value when used relative to FOXP3 levels in subgroups of GC patients. CD8/FOXP3 low and CD8/PD-L1 high signatures may reflecting a balance between tumor-reactive and immunosuppressive TIL subpopulations.

#### Validation of clustering signature using RNAseq data from TCGA cohort

To validate the survival prediction value of our patient clustering signature analysis in GC, we next analyzed RNA sequencing of GC samples from TCGA datasets ( $n = 375$  samples). We

tried two different combinations of these five predictors in the TCGA cohort, similar to what we did with the TMA data analysis. One combination used the 3 individual predictors including FOXP3, CD8 and PD-L1 (data not shown). The other combination used the 2 ratios including CD8/FOXP3 and CD8/PD-L1. We were unable to identify different immune signature subgroups, when solely relying on 3 individual predictors. Therefore, hierarchical clustering analyses relying on the ratio of CD8/FOXP3 and CD8/PD-L1 was applied to define the potential subgroups of patients from the TCGA cohort. As shown in Fig 6A, we were able to identify five groups of tumor tissues stratified according to their ratios of CD8/PD-L1 and CD8/FOXP3. Interestingly, three main groups (Cluster 1: low

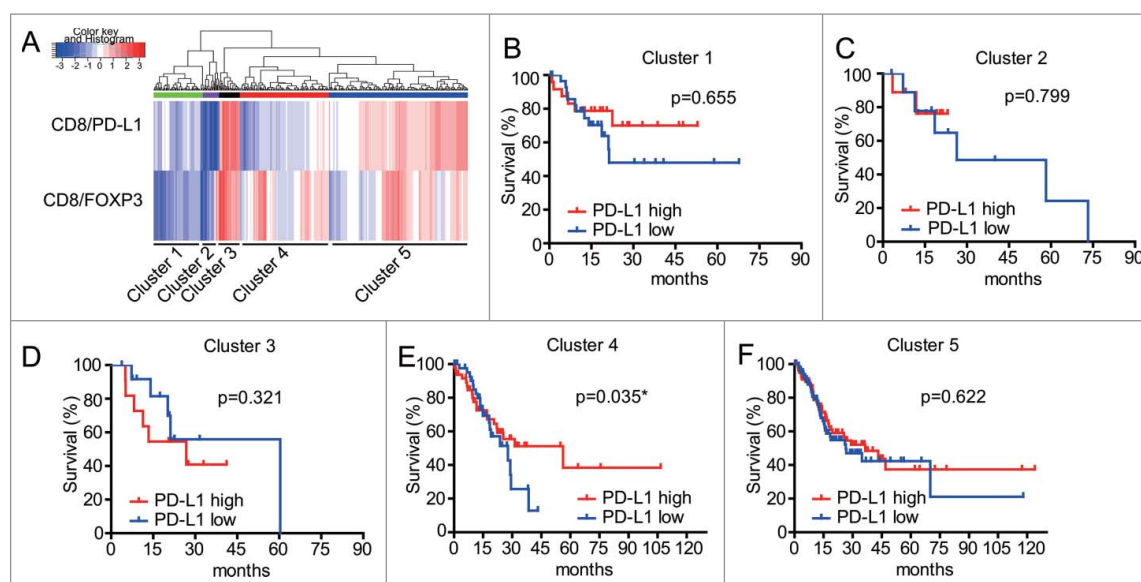


**Figure 6.** Kaplan-Meier analyses of overall survival (OS) for CD8/FOXP3 and CD8/PD-L1 in subgroups of patients from TCGA data. A. Hierarchical clustering of CD8/FOXP3 and CD8/PD-L1 of GC patients ( $n = 375$ ) from TCGA data. B-F Survival outcomes of the GC patients with different expression of PD-L1 in the 5 clusters generated according to their CD8/FOXP3 and CD8/PD-L1 ratios. Patients with higher PD-L1 expressions in Cluster 4 had significantly increased survival ( $p < 0.05$ ). Statistical analyses in Fig. 6E were generated using Fleming-Harrington test ( $p = 1, q = 1$ ) and other survival curves were analyzed using Log rank test.

CD8/FOXP3 ratio and low CD8/PD-L1 ratio, Cluster 4: high CD8/FOXP3 ratio and low CD8/PD-L1 ratio; and Cluster 5: high CD8/FOXP3 ratio and high CD8/PD-L1 ratio), exhibited a similar pattern to those observed in our mIHC TMA data (Fig. 4F). Critically, high expression of PD-L1 was associated with increased survival prognosis in patients from the Cluster 4 (exhibiting high CD8/FOXP3 ratio and low CD8/PD-L1 ratio) (Fig. 6E). This result was surprisingly consistent with the result from our mIHC TMA data. Nonetheless, PD-L1 levels did not show prognostic value in the remaining four patient subgroups (Fig. 6B, C, D, F). A summary table (Table 1) details the expression of these markers in tumor and adjacent normal tissues along with providing immune patterns in tumor tissues that related with patients' prognosis.

## Discussion

We have established a novel 4-color mIHC method that facilitates concurrent study of multiple parameters in gastric tissues, with the potential to illuminate our understanding of immune regulation within tumor microenvironment.<sup>20</sup> This technology

**Table 1.** Expression of FOXP3, PD-L1, CD8 and their ratios in adjacent normal and tumor tissues and the relationship with patients' prognosis.

Markers	Adjacent normal tissues	Tumor tissues
FOXP3 <sup>+</sup>	Low	High
PD-L1	Low	High
CD8 <sup>+</sup>	High	Low
CD8/FOXP3	High	Low
CD8/PD-L1	No significant difference	
Tissues	Better prognosis	Poor prognosis
Tumor tissues	High PD-L1 expression with low CD8/PD-L1 and high CD8/FOXP3	Low PD-L1 expression with low CD8/PD-L1 and high CD8/FOXP3
Tumor tissues	High CD8/PD-L1 and low CD8/FOXP3	Low CD8/PD-L1 and low CD8/FOXP3

may help overcome the current limitations of conventional single-color immunohistochemistry approaches used to classify patients, for instance based on either CD3<sup>+</sup> or CD8<sup>+</sup> T cell infiltration.<sup>21</sup> In support of this, our study revealed that the concurrent analysis of several immune cell populations can serve as a better survival predictor compared with CD8T cell alone. Critically, integration of data collected from our mIHC TMA cohort and TCGA cohort with unsupervised hierarchical clustering, allowed us to define the correlation expression patterns or density levels of CD8 T cells, FOXP3 Treg cells and PD-L1 levels in GC tumors.

We found that density levels of infiltrating FOXP3 Treg cells and PD-L1 expression were elevated in GC tissues, while CD8 cell populations were decreased. Nonetheless, the use of these immune markers, individually considered, failed to show any prognostic value in GC. We observed that the ratios of CD8/FOXP3 and, to a less extent, those of CD8/PD-L1 ratios were suppressed in tumor tissues. This led us to stratify our cohort of cancer patients into three groups according to their ratios of CD8/PD-L1 and CD8/FOXP3, and evaluate the prognostic value of PD-L1 expression in these subgroups. In these analyses, high levels of PD-L1 were associated with increased survival in patients with high ratios of CD8/FOXP3 and low ratios of CD8/PD-L1. Critically, this observation was reproduced in an independent cohort of patients from TCGA database. Conversely, patients with high CD8/FOXP3 and high CD8/PD-L1 ratios had poorer prognosis in our cohort of GC patients. These findings may be important to understand the success or failure of immunotherapies, and develop predictive biomarkers for the selection of patients with the highest likelihood of response to treatment.

Through the application of biomarker discovery and validation, CD8T cell infiltrates have been shown to have prognostic value in various types of cancers. High levels of CD8 and PD-L1 staining correlate with responses to anti-PD-L1 immunotherapy agents in renal cell carcinoma (RCC), melanoma and



non-small cell lung cancer (NSCLC).<sup>22</sup> However, patients with high levels of T cell infiltrates together with high intratumoral PD-L1 expression can also fail to respond to anti-PD-L1 therapy.<sup>23</sup> Indeed, complex tumor microenvironments are difficult to encapsulate with single markers such as CD8 and PD-L1.<sup>24</sup> Thus, the use of multiparametric analyses of immune cell types and checkpoints, such as CD8 T cells, FOXP3 Treg cells and PD-L1, may provide a more comprehensive picture of immune phenotypes within the tumor microenvironment, which may help stratify patients with the best chance of response to immunotherapies.

Immune response against the tumor is dependent on the proximity of lymphocytes to the tumor. The presence of tumor-infiltrating CD8T cells has previously been described in patients with advanced GC.<sup>25</sup> Such tumor-infiltrating CD8T cells can recognize and kill specific tumor-derived cells. However, in late-stage GC tumor regression, tumor-infiltrating lymphocytes (TILs) are rarely seen in the tumor microenvironment, suggesting that such TILs are more common in early-stage disease, and that advanced gastrointestinal malignancies are less immunogenic, presumably due to selection pressure operating during disease progression.<sup>26</sup> Multiple studies have shown that increased PD-L1 expression correlates with worse prognosis, highlighting the prognostic value of PD-L1 expression in GCs.<sup>18</sup> As such, elevated expression of PD-L1 is associated with advanced cancer stage increased nodal metastases and worse survival outcomes.<sup>19</sup> However, our data establish the need to incorporate the analysis of CD8 and FOXP3 levels to realize the full prognostic potential of PD-L1 in GC. Our data show that a subgroup of patients with high expression of PD-L1 together with high ratios of CD8/FOXP3 and low ratios of CD8/PD-L1, had increased survival. This suggests that PD-L1 may have augmented anti-tumorigenic activity in select gastric carcinoma patients through the modulation of specific immune interactions between CD8 and FOXP3 cells. Further studies may help define the mechanisms underlying these anti-tumorigenic actions of PD-L1.

The original aim of this study was to define whether the tumor microenvironment could be characterized through the concurrent analysis of three markers on four-micrometer-thick gastric disease tissue sections.<sup>27</sup> We found that the overall approach was technically reproducible and accurate. In addition to PD-L1, we also analyzed cell densities levels of CD8 and FOXP3 populations to measure the balance between anti-tumor lymphocytes and immunoregulatory/suppressive lymphocytes. This relied on the previous demonstration that high ratios of CD8/FOXP3 cells could be associated with favorable anti-tumor responses in a variety of solid tumors.<sup>28,29</sup> In addition to determining ratios of CD8/FOXP3, we also analyzed ratios of CD8/PD-L1 that reflect an escape of adaptive immune responses (i.e. where the antitumoral activity of pre-existing CD8 T cells located at the tumor margin is suppressed by PD-L1), and may help predict response to therapy.<sup>2</sup> In our study, the ratios of CD8/FOXP3 and CD8/PD-L1 were suppressed in tumor tissues. Using the CD8/PD-L1 ratio, we were able to classify the samples into three groups. Further integration of the CD8/FOXP3 ratio increased the complexity of the immune phenotypes, allowing us to define more subgroups of patients with different disease-risk (Fig. 4 F). This approach could be

replicated to define subgroups of GC patients in samples from a TCGA cohort (Fig. 6). Elevated tumor PD-L1 expression correlated with PD-1 inhibitor response rates in a recent phase I clinical trial (KEYNOTE-012/ anti-PD-1 monoclonal antibody pembrolizumab) in patients with advanced PD-L1 positive GC, which supported a trend towards improved overall response rate (ORR) and progression-free survival (PFS).<sup>30</sup> However, a few patients with lower responses to the PD-1 inhibitor treatment also had high levels PD-L1 expression.<sup>23</sup> We propose that our approach using concurrent CD8/FOXP3 and CD8/PD-L1 ratios to stratify patients into different risk subgroups may be useful for predicting the outcome of PD-1 inhibitor therapies in GC patients.

Our analyses also suggest that high CD8/FOXP3 ratios have favorable clinical outcomes, in line with several studies demonstrating an important role for CD8<sup>+</sup>FOXP3<sup>+</sup> Treg cells in tumor immune evasion.<sup>31</sup> Critically, high CD8/FOXP3 ratios together with high PD-L1 levels was associated with better survival in our GC patients. This finding is in agreement with a recent report that high levels of Tregs, denoted by the ratio of FOXP3/CD3 T-cells, was significantly associated with higher PD-L1 expression in metastatic lesions from renal carcinoma.<sup>32</sup> Additionally, we noticed that low ratios of CD8/FOXP3 were found to be predictive of increased survival in patients from selected clusters (Cluster 3, Fig. 5I). This signature is indicative of an escape of adaptive immune responses, and resulting in blunted immune surveillance.

In conclusion, we show that 4-color mIHC can be used to better define immune phenotypes in human GC. Our subgroup analyses indicate that the ratios of cytotoxic T cells to regulatory T cells (CD8/FOXP3) and cytotoxic T cells to PD-L1 (CD8/PD-L1) can predict anti-tumor interactions in the microenvironment. This suggests that the combined measure of CD8T cells, FOXP3 Treg cells and PD-L1 levels has more predictive potential than PD-L1 expression or CD8 levels alone. These findings may be important in understanding the mechanisms of immune evasion by the tumor, and the balance between cells with antitumoral activities and cells with immune suppressive activities. Our approach may also provide more accurate prognosis and help identify GC patients in which PD-L1 blockade therapy may be more effective.

## Disclosure of potential conflicts of interest

No potential conflicts of interest were disclosed.

## Acknowledgments

We are grateful to the staff at the Department of General Surgery at the Shanghai Jiao Tong University Affiliated First People's Hospital, and Ruijin Hospital for the collection of samples from the related patients.

## Funding

This work was supported by grants from the National Natural Science Foundation of China (81273247, 81472655 and 31670905) and the Shanghai Municipal Education Commission key discipline support project 2015-10101001-1. The National Health and Medical Research Council of Australia Grants (1066665) and the Australian Research Council (140100594 Future Fellowship to M.P.G.).

## Authors' contributions

**Conception and design:** L.Ying, F.Yan, D.Xu, Y.Hu

**Acquisition of data** (provided reagents, acquired and managed patients, provided facilities, etc.): Q.M, L.Yu, X.Yuan, B.Williams, D.Chan, L.Shi, P. Ni, X. Wang,

**Analysis and interpretation of data** (e.g., statistical analysis, biostatistics, computational analysis): L.Ying, F.Yan, D.Xu

**Writing, review, and/or revision of the manuscript:** L.Ying, F.Yan, M. Gantier, W.Chen, X.Zang, D.Xu, Y.Hu

**Administrative, technical, or material support** (i.e., reporting or organizing data, constructing databases): D.Xu, Y.Hu.

## ORCID

Le Ying  <http://orcid.org/0000-0002-8178-7874>

Feng Yan  <http://orcid.org/0000-0002-8848-1739>

Michael P. Gantier  <http://orcid.org/0000-0003-3740-698X>

## References

- Allemani C, Weir HK, Carreira H, Harewood R, Spika D, Wang XS, Bannon F, Ahn JV, Johnson CJ, Bonaventure A, et al. Global surveillance of cancer survival 1995–2009: analysis of individual data for 25,676,887 patients from 279 population-based registries in 67 countries (CONCORD-2). *Lancet*. 2015;385:977–1010. 10.1016/S0140-6736(14)62038-9. PMID:25467588.
- Tumeh PC, Harview CL, Yearley JH, Shintaku IP, Taylor EJ, Robert L, Chmielowski B, Spasic M, Henry G, Ciobanu V, et al. PD-1 blockade induces responses by inhibiting adaptive immune resistance. *Nature*. 2014;515:568–71. 10.1038/nature13954. PMID:25428505.
- Quail DF, Joyce JA. Microenvironmental regulation of tumor progression and metastasis. *Nat Med*. 2013;19:1423–37. 10.1038/nm.3394. PMID:24202395.
- Ajani JA, Lee J, Sano T, Janjigian YY, Fan D, Song S. Gastric adenocarcinoma. *Nat Rev Dis Primers*. 2017;3:17036. 10.1038/nrdp.2017.36. PMID:28569272.
- Shen LS, Wang J, Shen DF, Yuan XL, Dong P, Li MX, Xue J, Zhang FM, Ge HL, Xu D. CD4(+)CD25(+)CD127(low/-) regulatory T cells express Foxp3 and suppress effector T cell proliferation and contribute to gastric cancers progression. *Clin Immunol*. 2009;131:109–18. 10.1016/j.clim.2008.11.010. PMID:19153062.
- Yuan XL, Chen L, Li MX, Dong P, Xue J, Wang J, Zhang TT, Wang XA, Zhang FM, Ge HL, et al. Elevated expression of Foxp3 in tumor-infiltrating Treg cells suppresses T-cell proliferation and contributes to gastric cancer progression in a COX-2-dependent manner. *Clin Immunol*. 2010;134:277–88. 10.1016/j.clim.2009.10.005. PMID:19900843.
- Wen T, Wang Z, Li Y, Li Z, Che X, Fan Y, Wang S, Qu J, Yang X, Hou K, et al. A four-factor immunoscore system that predicts clinical outcome for stage II/III gastric cancer. *Cancer Immunol Res*. 2017;5:524–34. 10.1158/2326-6066.CIR-16-0381. PMID:28619967.
- Blankenstein T, Coulie PG, Gilboa E, Jaffee EM. The determinants of tumour immunogenicity. *Nat Rev Cancer*. 2012;12:307–13. 10.1038/nrc3246. PMID:22378190.
- Thompson ED, Zahurak M, Murphy A, Cornish T, Cuka N, Abdelfatah E, et al. Patterns of PD-L1 expression and CD8 T cell infiltration in gastric adenocarcinomas and associated immune stroma. *Gut*. 2017;66:794–801. 10.1136/gutjnl-2015-310839. PMID:26801886.
- Apetoh L, Smyth MJ, Drake CG, Abastado JP, Apte RN, Ayyoub M, Blay JY, Bonneville M, Butterfield LH, Caignard A, et al. Consensus nomenclature for CD8+ T cell phenotypes in cancer. *Oncoimmunology*. 2015;4:e998538. 10.1080/2162402X.2014.998538. PMID:26137416.
- Fu J, Xu D, Liu Z, Shi M, Zhao P, Fu B, Zhang Z, Yang H, Zhang H, Zhou C, et al. Increased regulatory T cells correlate with CD8 T-cell impairment and poor survival in hepatocellular carcinoma patients. *Gastroenterology*. 2007;132:2328–39. 10.1053/j.gastro.2007.03.102. PMID:17570208.
- Yuan X, Yu L, Li J, Xie G, Rong T, Zhang L, Chen J, Meng Q, Irving AT, Wang D, et al. ATF3 suppresses metastasis of bladder cancer by regulating gelsolin-mediated remodeling of the actin cytoskeleton. *Cancer Res*. 2013;73:3625–37. 10.1158/0008-5472.CAN-12-3879. PMID:23536558.
- Yan F, Ying L, Li X, Qiao B, Meng Q, Yu L, Yuan X, Ren ST, Chan DW, Shi L, et al. Overexpression of the transcription factor ATF3 with a regulatory molecular signature associates with the pathogenic development of colorectal cancer. *Oncotarget*. 2017;8:47020–36. PMID:28402947.
- tack EC, Wang C, Roman KA, Hoyt CC. Multiplexed immunohistochemistry, imaging, and quantitation: a review, with an assessment of Tyramide signal amplification, multispectral imaging and multiplex analysis. *Methods*. 2014;70:46–58. 10.1016/j.jymeth.2014.08.016. PMID:25242720.
- Sadler AJ, Rossello FJ, Yu L, Deane JA, Yuan X, Wang D, Irving AT, Kaparakis-Liaskos M, Gantier MP, Ying H, et al. BTB-ZF transcriptional regulator PLZF modifies chromatin to restrain inflammatory signaling programs. *Proc Natl Acad Sci U S A*. 2015;112:1535–40. 10.1073/pnas.1409728112. PMID:25605927.
- Zhang M, Dong Y, Liu H, Wang Y, Zhao S, Xuan Q, Wang Y, Zhang Q. The clinicopathological and prognostic significance of PD-L1 expression in gastric cancer: a meta-analysis of 10 studies with 1,901 patients. *Scientific Reports*. 2016;6:37933. 10.1038/srep37933. PMID:27892511.
- Qing Y, Li Q, Ren T, Xia W, Peng Y, Liu GL, Luo H, Yang YX, Dai XY, Zhou SF, et al. Upregulation of PD-L1 and APE1 is associated with tumorigenesis and poor prognosis of gastric cancer. *Drug Design Dev Therapy*. 2015;9:901–9. 10.2147/DDDT.S75152. PMID:25733810.
- Saito H, Kuroda H, Matsunaga T, Osaki T, Ikeguchi M. Increased PD-1 expression on CD4+ and CD8+ T cells is involved in immune evasion in gastric cancer. *J Surg Oncol*. 2013;107:517–22. 10.1002/jso.23281. PMID:23129549.
- Hou J, Yu Z, Xiang R, Li C, Wang L, Chen S, Li Q, Chen M, Wang L. Correlation between infiltration of FOXP3+ regulatory T cells and expression of B7-H1 in the tumor tissues of gastric cancer. *Exp Mol Pathol*. 2014;96:284–91. 10.1016/j.yexmp.2014.03.005. PMID:24657498.
- Kalra J, Baker J. Multiplex Immunohistochemistry for Mapping the Tumor Microenvironment. *Methods Mol Biol*. 2017;1554:237–51. 10.1007/978-1-4939-6759-9\_17. PMID:28185197.
- Zhang W, Hubbard A, Jones T, Racolta A, Bhumik S, Cummins N, Zhang L, Garsha K, Ventura F, Lefever MR, et al. Fully automated 5-plex fluorescent immunohistochemistry with tyramide signal amplification and same species antibodies. *Lab Invest*. 2017;97(7):873–885. 10.1038/labinvest.2017.37. PMID:28504684.
- Chinai JM, Janakiram M, Chen F, Chen W, Kaplan M, Zang X. New immunotherapies targeting the PD-1 pathway. *Trends Pharmacol Sci*. 2015;36:587–95. 10.1016/j.tips.2015.06.005. PMID:26162965.
- Kim JM, Chen DS. Immune escape to PD-L1/PD-1 blockade: seven steps to success (or failure). *Annals Oncol Official J Eur Soc Medical Oncol*. 2016;27:1492–504. 10.1093/annonc/mdw217. PMID:27207108.
- Colwell J. Is PD-L1 expression a biomarker of response? *Cancer Discovery*. 2015;5:1232. 10.1158/2159-8290.CD-ND2015-004. PMID:26516064.
- Turcotte S, Gros A, Tran E, Lee CC, Wunderlich JR, Robbins PF, Rosenberg SA. Tumor-reactive CD8+ T cells in metastatic gastrointestinal cancer refractory to chemotherapy. *Clin Cancer Res*. 2014;20:331–43. 10.1158/1078-0432.CCR-13-1736. PMID:24218514.
- DuPage M, Mazumdar C, Schmidt LM, Cheung AF, Jacks T. Expression of tumour-specific antigens underlies cancer immunoeediting. *Nature*. 2012;482:405–9. 10.1038/nature10803. PMID:22318517.
- Ying L, Yan F, Meng Q, Yuan X, Yu L, Williams BRG, Chan DW, Shi L, Tu Y, Ni P, et al. Understanding immune phenotypes in human gastric disease tissues by multiplexed immunohistochemistry. *J Translational Med*. 2017;15:206. 10.1186/s12967-017-1311-8. PMID:29025424.
- Salama P, Phillips M, Grieu F, Morris M, Zeps N, Joseph D, Platell C, Iacopetta B. Tumor-infiltrating FOXP3+ T regulatory cells show strong prognostic significance in colorectal cancer. *J Clin Oncol*. 2009;27:186–92. 10.1200/JCO.2008.18.7229. PMID:19064967.
- deLeeuw RJ, Kost SE, Kakal JA, Nelson BH. The prognostic value of FoxP3+ tumor-infiltrating lymphocytes in cancer: a critical review of the literature. *Clin Cancer Res*. 2012;18:3022–9. 10.1158/1078-0432.CCR-11-3216. PMID:22510350.

30. Muro K, Chung HC, Shankaran V, Geva R, Catenacci D, Gupta S, Eder JP, Golan T, Le DT, Burtneß B, et al. Pembrolizumab for patients with PD-L1-positive advanced gastric cancer (KEYNOTE-012): a multicentre, open-label, phase 1b trial. *Lancet Oncol.* 2016;17:717–26. 10.1016/S1470-2045(16)00175-3. PMID:27157491.
31. Kiniwa Y, Miyahara Y, Wang HY, Peng W, Peng G, Wheeler TM, Thompson TC, Old LJ, Wang RF. CD8+ Foxp3+ regulatory T cells mediate immunosuppression in prostate cancer. *Clin Cancer Res.* 2007;13:6947–58. 10.1158/1078-0432.CCR-07-0842. PMID:18056169.
32. Baine MK, Turcu G, Zito CR, Adeniran AJ, Camp RL, Chen L, Kluger HM, Jilaveanu LB. Characterization of tumor infiltrating lymphocytes in paired primary and metastatic renal cell carcinoma specimens. *Oncotarget.* 2015;6:24990–5002. 10.18632/oncotarget.4572. PMID:26317902.